Palestinian Medical and Pharmaceutical Journal

Trifluorooxoacetamido Benzamides as Breakthrough CETP Inhibitors: A Synergistic Approach of Synthesis, Biological Assessment, and Molecular Modeling

Reema Abu Khalaf[1,*], Areej NasrAllah[1], Dima Sabbah[1], Balqis Ikhmais[1], Ghadeer AlBadawi[1] & Maha Awad[1]

Type: Full Article. Received: 17th Feb. 2025, Accepted: 1st Jun. 2025 Published: ××××, DOI: ××××

Abstract: Cardiovascular diseases are the first leading cause for death in the United States and the third globally. Cholesteryl ester transfer protein (CETP) is a glycoprotein excreted mainly from the liver and transfers cholesteryl esters from high-density lipoproteins to low-density lipoproteins. Inhibition of CETP activity decreases lipid transfers, which raises high-density lipoprotein cholesterol and lowers that of low-density lipoproteins. Cardiovascular risk is decreased when CETP activity is inhibited. There is a growing need for new CETP inhibitors which encourages us to conduct this research. In this work, synthesis of eighteen new trifluoro-oxoacetamido benzamides **9a**-**r** was carried out by nucleophilic acyl substitution reaction to form the amide followed by characterization of the prepared derivatives using ^{1}H-NMR, ^{13}C-NMR and IR spectroscopy. *In vitro* study showed that the synthesized compounds **9a**-**r** exhibited distinguished activity against CETP with IC_{50} values ranging from 1.24 µM to 7.16 × 10^{-8} µM, where compound **9l** had the best activity. Induced-fit docking results illustrated that torcetrapib, anacetrapib, and **9a**-**r** accommodated CETP binding cleft and that hydrophobic force predominated the inhibitor/CETP complex formation. Additionally, they bonded to C13, Q199, R201, and H232 residues through H-bond. ΔG of the verified analogues surpassed that of co-crystallized ligand (0RP) and anacetrapib anticipating the matching of analogues' core structures to CETP key binding residues. Moreover, inhibitors **9a**-**r** mapped the pharmacophore model's fingerprint of CETP active inhibitors and subsequently elaborated the binding score values against CETP binding domain.

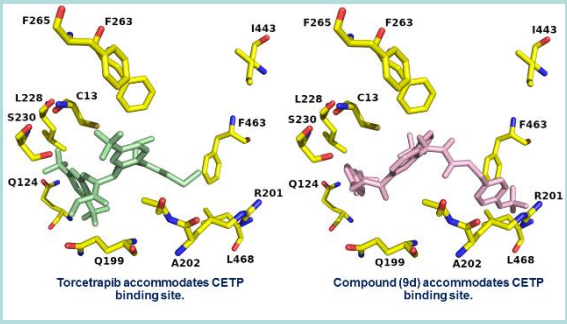

Keywords: Benzamides, CETP, Induced-fit docking, Inhibitors, Pharmacophore, Trifluoro-oxoacetamido.

Introduction

Cardiovascular disease (CVD) is a common cause of morbidity and mortality in patient with dyslipidemia [1]. CVD risk factors are high blood pressure, smoking, diabetes, physically inactive, obesity, high level of low density lipoprotein (LDL) cholesterol (bad cholesterol), and low level of high density lipoprotein (HDL) cholesterol (good cholesterol) [2]. In order to alleviate the worldwide burden of atherosclerotic cardiovascular disease, it is imperative to reduce low-density lipoprotein (LDL). Apart from dietary and lifestyle changes, the development of pharmacotherapies to lower LDL is making it possible to lower LDL even further and reduce the risk of CVD [3, 4].

Cholesteryl ester transfer protein (CETP) is the key transfer protein that is responsible for handover of cholesteryl esters and triglycerides between the lipoprotein particles in order to assist in the collection of triglycerides from very low density lipoproteins (VLDL) or LDL and exchanges them for cholesteryl esters from HDL and *vice versa* [5]. This mechanism is vital for maintaining lipid homeostasis, particularly in regulating cholesterol transport and the development of atherosclerosis [6]. CETP's activity notably affects the size and the composition of HDL particles, due to their role in reverse cholesterol transport and cardiovascular protection [7].

The connection between CETP and cardiovascular diseases is well-established, with heightened CETP activity linked to lower HDL cholesterol levels and an elevated risk of atherosclerosis and coronary artery disease [8]. In fact, the invention of CETP inhibitors aroused when it was discovered that some human lack of CETP naturally owing to the absence of the responsible gene. Remarkably the human with CETP deficiency has high levels of HDL, low levels of LDL and significantly reduced CVD chance [3, 9]. Throughout the CETP inhibition trials with torcetrapib, which had been abruptly stopped in the clinical stages, clinical benefit was not demonstrated in cardiovascular outcomes even with other CETP inhibitors. However, these failures were caused by compound-related problems, such as adverse effects with torcetrapib, insufficient LDL cholesterol lowering with dalcetrapib, and inadequate follow-up duration for the amount of LDL cholesterol lowering produced by evacetrapib [10]. Anacetrapib, and evacetrapib decreased the relative risk for developing diabetes, whereas patients treated with torcetrapib showed reductions in plasma glucose and insulin [11]. Although

[1] Department of Pharmacy, Faculty of Pharmacy, Al-Zaytoonah University of Jordan, Amman, Jordan.
Corresponding author email: reema.abukhalaf@zuj.edu.jo; ORCID ID: https://orcid.org/0000-0002-7797-8918.

torcetrapib and evacetrapib were shown to boost the cholesterol efflux capability of total HDL, neither of them decreased cardiovascular events [12].

Notably, a pivotal study revealed the compelling ability of obicetrapib, alongside a statin and ezetimibe substantially enhance beneficial HDL cholesterol and markedly diminish harmful LDL cholesterol atherogenicity [13]. Consequently, the effective modulation of lipid levels offers a powerful means to significantly improve the health outcomes of individuals with dyslipidemia [14]. Therefore, a significant focus in pharmacological research has been the targeting of CETP as a promising new avenue for decisively reducing the incidence of CVD through the identification of potent inhibitors.

Our research group had previously prepared various prospective CETP inhibitors such as: benzylidene-amino methanones [15], benzyl- amino-methanones [16], *N*-(4-benzyloxyphenyl)-4-methyl-benzenesulfonamides [17], *N*-(4-benzylamino- phenyl)-toluene-4-sulfonic acid esters [17], chlorobenzyl benzamides [18], fluorinated benzamides [19], and other substituted benzyl benzamides [20-24]. In the current work, we aimed to improve the CETP inhibitory activity of the lead compounds **A** [20] and **B** [18] presented in Figure **1,** in addition to further explore the structure-activity relationship of this series of CETP inhibitors. Herein, new eighteen oxoacetamido-benzamides **9a**-**r** were prepared by replacing the *p*-F and *p*-Cl aromatic ring substitutions of **A** and **B** with *p*-OCF_3, *o*-OCH_3, *o*-F, *o*-CF_3, *m*-CF_3, and 3,5-bis-CF_3 groups, as well as varying *p*-OCF_3 (in **B**) or 3,5-bis-CF_3 (in **A**) moieties with *p*-CF_3 group. Afterward, *in vitro* biological evaluation was carried out to determine the effect of these structural modifications, for both the nature and position of the aromatic ring substitution, on the CETP inhibitory activity. Furthermore, induced-fit docking (IFD) studies were executed for compounds **9a**-**r** against the coordinates of CETP binding domain so as to explain the structural-basis of binding of these inhibitors. Whereas, the binding free energy of CETP receptor and ligand complex was calculated using Prime MMGBSA. Pharmacophore mapping of compounds **9a**-**r** against a recorded pharmacophore model of active CETP inhibitors was also conceded.

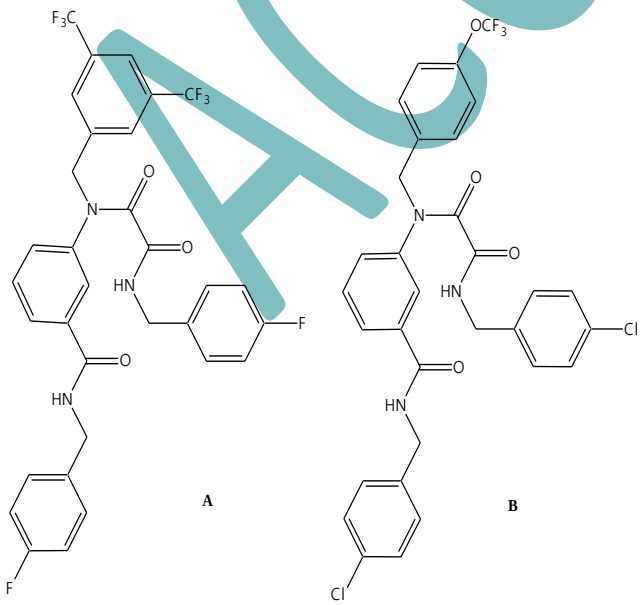

Figure (1): Structures of formerly synthesized hit compounds: **A** (IC_{50}= 1.30 µM), and **B** (IC_{50}= 1.60 µM) [18, 20].

Materials and Methods

Chemicals Materials

All compounds and solvents were of laboratory grade and used without extra purification. Chemicals and solvents were purchased from the corresponding companies (Alfa Aesar, Acros Organics, Sigma–Aldrich, Fluka, SD Fine Chem Limited, Tedia and Fisher Scientific). CETP fluorometric assay kit II was obtained from MyBioSource, USA. Pre-coated Thin Layer Chromatography (TLC) plates were performed on 20×20 cm, 0.20 mm silica gel 60 with fluorescent indicator UV at 254 nm (Macherey-Nagel, Germany). Also, TLC was performed on 20×20 cm aluminum plates pre-coated with fluorescent silica gel GF254 (Macherey-Nagel, Germany) and envisioned by UV light (at 254 and/ or 360 nm). Column chromatography was used on silica gel stationary phase of high-purity grade, pore size 60 A°, 70-230 mesh, 63-20µm (Sigma-Aldrich, Germany).

Instruments

Shimadzu IR Affinity1 FT-IR spectrophotometer was used for measuring IR spectra at Al-Zaytoonah University of Jordan. Bruker, Avance DPX- 500 spectrometer, was used to record ^{13}C-NMR and ^{1}H-NMR spectra, The University of Jordan. Biological study of the prepared compounds was completed by FLX800TBI Microplate Fluorimeter (BioTek, USA).

Synthesis of intermediates 5a, 5b and 5c.

Elaboration of 3-aminobenzoic acid methyl ester (**3**) was achieved as reported prior [18-20]. Then the methyl benzoate intermediates **5a, 5b** were synthesized as previously described [18-20]. Synthesis of **5c** started by adding 2.0 g (13.2 mmol) of ester **3** to 20 ml dichloromethane (DCM). After that 1-(bromomethyl)-4-(trifluoromethyl) benzene (**4c**, 6.14 ml, 39.6 mmol), and triethylamine (TEA, 9.3 ml, 66.2 mmol) were appended. The combination was left under stirring at room temperature for 5 days then the solution was vaporized and the intermediate methyl 3-(4-(trifluoromethyl) benzylamino) benzoate (**5c**) was refined by column chromatography using cyclohexane: ethyl acetate (9:1) as eluent. Intermediate **5c** was obtained as a yellow powder (3.19 g, % yield = 78%); $C_{16}H_{14}F_3NO_2$; mp. 126-127°C; R_f= 0.4 (cyclohexane: ethyl acetate, 9:1); ^{1}H-NMR (500 MH_Z, DMSO-d6): δ 3.30-3.39 (m, 1H, CH_2NH), 3.79 (s, 3H, OCH_3), 4.42 (d, *J* = 6.0 H_Z, 2H, CH_2), 6.74 (t, *J* = 7.8 H_Z, 1H, Ar-*H*), 6.80 (d, *J* = 7.8 H_Z, 1H, Ar-*H*), 7.14-7.21 (m, 2H, Ar-*H*), 7.57 (d, *J* = 8.0 H_Z, 2H, Ar-*H*), 7.69 (d, *J* = 8.1 Hz, 2H, Ar-*H*) ppm; ^{13}C-NMR (125 MH_Z, DMSO-d6): δ 46.3, 52.4, 113.2, 117.1, 117.2, 123.7, 125.6, 125.9, 128.2, 129.7, 130.8, 145.4, 149.0, 167.1 ppm; IR (KBr): 3394, 3039, 2962, 1712, 1612, 1527, 1334, 1257, 1157 cm^{-1}.

Synthesis of compounds 9a-r

Elaboration of the acyl intermediate **7a, 7b** from **5a, 5b** was done as formerly stated [18-20]. While the methyl 3-(4-(trifluoromethyl) benzylamino) benzoate (**5c**, 0.25 g) was hydrolyzed to the benzoic acid **6c** as reported earlier [18-20]. Subsequently, **6c** (0.2 g, 0.64 mmol) was dissolved in 10 ml DCM and then oxalyl chloride (**2**, 0.11 ml, 1.2 mmol, $(COCl)_2$) was added. The reaction remained under agitation for 4 days at 60-70 ºC. Later the reaction combination was vaporized to achieve the acyl intermediate **7c**.

N-(2-Fluorobenzyl)-3-(2-(2-fluorobenzylamino)-N-(4-(trifluoromethoxy)benzyl)-2-oxoacetamido)benzamide (9a)

(2-Fluorophenyl)methanamine (**8a**, 0.155 ml, 1.37 mmol) together with 5 ml of TEA and 10 ml of DCM were added to **7a** (0.64 mmol), then the reaction combination was mixed at room temperature for 5 days. Then the product was purified by column chromatography using cyclohexane: ethyl acetate, 65:35 as eluent. Viscous compound was gained **9a** (0.057 g, % yield = 15%); $C_{31}H_{24}F_5N_3O_4$; R***f*** = 0.56 (cyclohexane: ethyl acetate, 65:35); ^{1}H-NMR (500 MH_Z, DMSO-d6): δ 4.09 (d, *J* = 5.3 H_Z, 2H, COCOHNCH_2), 4.43 (d, *J* = 5.0 H_Z, 2H, COHNCH_2), 5.04 (s, 2H, NCH_2), 6.83 (t, *J* = 7.5 H_Z 1H, Ar-*H*), 6.95 (t, *J* = 7.95 H_Z, 1H, Ar-*H*), 7.12 (m, 4H, Ar-*H*), 7.30 (t, *J* = 7.45 H_Z , 4H, Ar-*H*), 7.43 (d, *J* = 8.05 H_Z, 2H, Ar- *H*), 7.60 (d, *J* = 7.9 H_Z , 2H, Ar- *H*), 7.78 (d, *J* = 7.6 Hz, 1H, Ar*H*), 7.83 (s, 1H, Ar- *H*), 9.00 (t, *J* = 5.53 Hz, 1H, N*H*), 9.18 (t, *J* = 5.0 Hz, 1H, N*H*); ^{13}C-NMR (125 MH_Z, DMSO-d6): δ 41.9, 43.1, 51.4, 123.7, 125.5, 126.9, 127.0, 127.1, 127.2, 127.4, 127.5, 128.3, 128.4, 128.5, 128.8, 128.9, 135.8, 138.5, 139.4, 139.8, 139.9, 141.0, 141.8, 163.4, 164.1, 165., 165.5, 167.4 ppm; IR (KBr): 3315, 3071, 2969, 2916, 2907, 2848, 1683, 1635,1456 cm^{-1}.

N-(2-Fluorobenzyl)-3-(2-(2-fluorobenzylamino)-N-(3,5-bis(trifluoromethyl)benzyl)-2-oxoacetamido)benzamide(9b)

(2-Fluorophenyl) methanamine (**8a**, 0.155 ml, 1.37 mmol) together with 5 ml of TEA and 10 ml of DCM were added to **7b** (0.64 mmol), then the reaction solution was agitated at room temperature for 5 days. Then the product was obtained by column chromatography using chloroform: methanol, 98: 2 as eluent. Viscous compound was gained **9b** (0.137 g, % yield = 33%); $C_{32}H_{23}F_8N_3O_3$; R***f*** = 0.4 (chloroform: methanol, 98: 2); ^{1}H-NMR (500 MH_Z, DMSO-d6): δ 4.17 (d, *J* = 6.85 Hz, 2H, COCOHNCH_2), 4.51 (d, *J* = 6.55 Hz, 2H, COHNCH_2), 5.19 (s, 2H, NCH_2), 6.77 (t, *J* = 7.2 Hz, 1H, Ar-*H*), 6.97 (t, *J* = 8.2 Hz, 1H, Ar-*H*), 7.09-7.38 (m, 7H, Ar-*H*), 7.82 (s, 2H, Ar-*H*), 7.84 (s, 2H, Ar-*H*), 7.90 (s, 1H, Ar-*H*), 8.02 (s, 1H, Ar-*H*), 9.01 (t, *J* = 6.85 Hz, 1H, N*H*), 9.3 (t, *J* = 6.55 H_Z, 1H, N*H*) ppm; ^{13}C-NMR (125 MH_Z, DMSO-d6): δ 35.8, 36.9, 50.8, 115.3, 115.4, 115.5, 115.6, 121.8, 124.7, 126.3, 126.4, 126.6, 127.0, 129.4, 129.6, 130.0, 130.5, 130.9, 135.7, 140.4, 140.6, 163.3, 165.5, 165.6 ppm; IR (KBr): 3386, 3258, 3100, 2963, 1684, 1587, 1490, 1457 cm^{-1}.

N-(2-Fluorobenzyl)-3-(2-(2-fluorobenzylamino)-N-(4-(trifluoromethyl)benzyl)-2-oxoacetamido)benzamide (9c)

(2-Fluorophenyl) methanamine (**8a**, 0.155 ml, 1.37 mmol) together with 5 ml of TEA and 10 ml of DCM were added to **7c** (0.64 mmol), then the reaction solution was agitated at room temperature for 5 days. Then the product was obtained by column chromatography using chloroform: methanol, 98: 2 as eluent. White powder was gained **9c** (0.195 g, % yield = 52.5 %); $C_{31}H_{24}F_5N_3O_3$; m.p = 145°-146°; R***f*** = 0.67 (chloroform: methanol, 98:2); ^{1}H-NMR (500 MH_Z, DMSO-d6): δ 4.17 (d, *J* = 5.45 H_Z, 2H, COCOHNCH_2), 4.51 (d, *J* = 5.35 H_Z, 2H, COHNCH_2), 5.09 (s, 2H, NCH_2), 6.78 (t, *J* = 7.35 H_Z 1H, Ar-*H*), 6.96-7.00 (t, *J* = 7.35 H_Z, 1H, Ar-*H*), 7.07-7.23 (m, 4H, Ar-*H*), 7.31-7.36 (t, *J* = 7.45 H_Z, 4H, Ar-*H*), 7.49 (d, *J* = 8.05 Hz, 2H, Ar-*H*), 7.68 (d, *J* = 7.9 Hz, 2H, Ar- *H*), 7.81 (d, *J* = 3.28 Hz, 1H, Ar- *H*), 7.87 (s, *J* = 7.6 Hz, 1H, Ar*H*), 9.03 (t, *J* = 5.85 Hz, 1H, N*H*), 9.27 (t, *J* = 10.9 Hz, 1H, N*H*); ^{13}C-NMR (125 MH_Z, DMSO-d6): δ 35.8, 37.0, 51.3, 115.3, 115.5, 115.65, 124.7, 125.04, 125.8, 126.3, 126.4, 126.6, 126.9, 129.1, 129.4, 129.6, 130.0, 130.6, 135.5, 140.9, 159.6, 161.5,163.5, 165.4, 165.7 ppm; IR (KBr): 3365, 3266, 3071, 2963,1694, 1641,1560 cm^{-1}.

N-(4-(Trifluoromethoxy)benzyl)-3-(N-(4-(trifluoromethoxy)benzyl)-2-(4-(trifluoromethoxy)benzylamino)-2-oxoacetamido)benzamide (9d)

(4-(Trifluoromethoxy)phenyl) methanamine (**8b**, 0.155 ml, 1.37 mmol) together with 5 ml of TEA and 10 ml of DCM were added to **7a** (0.64 mmol), then the reaction mixture was stirred at room temperature for 5 days. Then the crude product was purified by column chromatography using chloroform: methanol, 98: 2 as eluent. White powder was obtained **9d** (0.069 g, % yield = 15 %); $C_{33}H_{24}F_9N_3O_6$; m.p = 115-116°; R_f = 0.68 (chloroform: methanol, 98: 2), ^{1}H-NMR (500 MH_Z, DMSO-d6): δ 4.13 (d, *J* = 5.8 Hz, 2H, COCOHNCH_2), 4.45 (d, *J* = 5.7 Hz, 2H, COHNCH_2), 4.97 (s, 2H, NCH_2), 6.95 (d, *J* = 8.4 Hz, 2H, Ar-*H*), 7.11 (d, *J* = 8.05 Hz, 2H, Ar-*H*), 7.26 (d, *J* = 7.85 Hz, 5H, Ar-*H*), 7.33 (d, *J* = 8.5 Hz, 3H, Ar-*H*), 7.38 (d, *J* = 8.55 Hz, 3H, Ar-*H*), 7.79 (s, 1H, Ar-*H*), 9.08 (t, *J* = 5.8 Hz, 1H, N*H*), 9.25 (t, *J* = 5.7 H_Z, 1H, N*H*) ppm; ^{13}C-NMR (125 MH_Z, DMSO-d6): δ 41.3, 42.5, 51.1, 121.2, 121.4, 121.5, 126.8, 129.3, 129.5, 130.3, 131.0, 135.6, 136.1, 138.1, 139.4, 147.6, 148.0, 163.4, 165.3), 166.2 ppm; IR (KBr): 3375, 3312, 2965, 1696, 1657, 1515 cm^{-1}.

3-(N-(3,5-Bis(trifluoromethyl)benzyl)-2-(4-(trifluoromethoxy)benzylamino)-2-oxoacetamido)-N-(4-(trifluoromethoxy)benzyl)benzamide (9e)

(4-(Trifluoromethoxy)phenyl) methanamine (**8b**, 0.155 ml, 1.37 mmol) together with 5 ml of TEA and 10 ml of DCM were added to **7b** (0.64 mmol), then the reaction mixture was stirred at room temperature for 5 days. Then the crude product was purified by column chromatography using chloroform: methanol, 98: 2 as eluent. White powder was obtained **9e** (0.159 g, % yield = 32 %); $C_{34}H_{23}F_{12}N_3O_5$; R_f = 0.74 (chloroform: methanol, 98: 2), ^{1}H-NMR (500 MH_Z, DMSO-d6): δ 4.16 (d, *J* = 5.85 Hz, 2H, COCOHNCH_2), 4.47 (d, *J* = 5.75 Hz, 2H, COHNCH_2), 5.17 (s, 2H, NCH_2), 6.97 (d, *J* = 8.5 , 2H, Ar-*H*), 7.13 (d, *J* = 8.1 Hz, 2H, Ar-*H*), 7.26 (d, *J* = 6.30 Hz, 3H, Ar-*H*), 7.38 (d, *J* = 6.30 Hz, 3H, Ar-*H*), 7.82 (d, *J* = 8.41 Hz, 2H, Ar-*H*), 7.88 (d, *J* = 8.2 Hz, 2H, Ar-*H*), 7.98 (s, 1H, Ar-*H*), 9.10 (t, *J* = 5.85 Hz, 1H, N*H*), 9.32 (t, *J* = 5.75 H_Z, 1H, N*H*) ppm; ^{13}C-NMR (100 MH_Z, DMSO-d6): δ 42.7, 43.4, 54.2, 121.3, 121.4, 121.5, 126.9, 129.5, 129.7, 130.5, 131.5, 135.7, 136.3, 138.4, 139.6, 147.8, 148.2,148.0, 163.6, 165.5, 166.2 ppm; IR (KBr): 3369, 3217, 3077, 2966, 1691,1637,1510 cm^{-1}.

N-(4-(Trifluoromethoxy)benzyl)-3-(2-(4-(trifluoromethoxy)benzylamino)-N-(4-(trifluoromethyl)benzyl)-2-oxoacetamido)benzamide (9f)

(4-(Trifluoromethoxy)phenyl)methanamine (**8b**, 0.155 ml, 1.37 mmol) together with 5 ml of TEA and 10 ml of DCM were added to **7c** (0.64 mmol), then the reaction mixture was stirred at room temperature for 5 days. Then the crude product was purified by column chromatography using chloroform: methanol, 98: 2 as eluent. Off white powder was obtained **9f** (0.114 g, % yield = 25 %); $C_{33}H_{24}F_9N_3O_5$; m.p = 98°-99°; R***f*** = 0.6 (chloroform: methanol, 98: 2); ^{1}H-NMR (300 MH_Z, $CDCl_3$-d6): δ 4.29 (d, *J* = 5.9 Hz, 2H, COCOHNCH_2), 4.58 (d, *J* = 5.8 Hz, 2H, COHNCH_2), 4.96 (s, 2H, NCH_2), 6.45 (s, 1H, Ar-*H*), 7.13-7.32 (m, 11H, Ar-*H*), 7.52 (d, *J* = 6.0 Hz, 2H, Ar-*H*), 7.61 (d, *J* = 6.0 Hz, 2H, Ar-*H*), 9.11 (t, *J* = 5.9 Hz, 1H, N*H*), 9.25 (t, *J* = 5.8 H_Z, 1H, N*H*) ppm;

^{13}C-NMR (75 MH_Z, DMSO-d6): δ 42.7, 43.5, 54.5, 121.3, 121.4, 125.7, 125.9, 129.1, 129.2, 129.4, 129.5, 130.1, 134.5, 135.7, 136.7, 139.5, 148.7, 159.8, 162.0, 166.1 ppm; IR (KBr): 3348, 3271, 3078, 2963, 1667, 1512, 1327 cm^{-1}.

N-(3-(Trifluoromethyl)benzyl)-3-(2-(3-(trifluoromethyl)benzylamino)-N-(4-(trifluoromethoxy)benzyl)-2-oxoacetamido)benzamide (9g)

(3-(Trifluoromethyl)phenyl)methanamine (**8c**, 0.155 ml, 1.37 mmol) together with 5 ml of TEA and 10 ml of DCM were added to **7a** (0.64 mmol), then the reaction mixture was stirred at room temperature for 5 days. Then the crude product was purified by column chromatography using chloroform: methanol, 98: 2 as eluent. Viscous compound was obtained **9g** (0.059 g, % yield = 13.3 %); $C_{33}H_{24}F_9N_3O_4$; R_f = 0.7 (chloroform: methanol, 98: 2), ^{1}H-NMR (500 MH_Z, DMSO-d6): δ 2.51 (s, 2H, COCOHNCH_2), 4.58 (d, J = 5.8 H_Z, 2H, COHNCH_2), 5.15 (s, 2H, NCH_2), 7.29 (s, 2H, Ar-H), 7.49- 7.90 (m, 12H, Ar-H), 8.01 (s, 1H, Ar-H), 8.22 (s, 1H, Ar-H), 8.74 (t, J = 6.9 Hz, 1H, NH), 9.16 (t, J = 5.7 H_Z, 1H, NH) ppm; ^{13}C-NMR (125 MH_Z, DMSO-d6): δ 42.8, 46.4, 51.5, 121.5, 121.8, 124.1, 124.3, 125.4, 125.9, 129.6, 129.9, 130.2, 131.9, 135.8, 136.8, 141.2, 141.4, 147.8, 163.1, 164.2, 166.1 ppm; IR (KBr): 3367, 3086, 2962, 1670, 1545 cm^{-1}.

3-(N-(3,5-Bis(trifluoromethyl)benzyl)-2-(3-(trifluoromethyl)benzylamino)-2-oxoacetamido)-N-(3(trifluoromethyl)benzyl)benzamide (9h)

3-(Trifluoromethyl)phenyl)methanamine (**8c**, 0.155 ml, 1.37 mmol) together with 5 ml of TEA and 10 ml of DCM were added to **7b** (0.64 mmol), then the reaction mixture was stirred at room temperature for 5 days. Then the crude product was purified by column chromatography using chloroform: methanol, 98: 2 as eluent. Viscous compound was obtained **9h** (0.119 g, % yield = 25 %); $C_{34}H_{23}F_{12}N_3O_3$; R_f = 0.65 (chloroform: methanol, 98: 2), ^{1}H-NMR (300 MH_Z, DMSO-d6): δ 4.19 (s, 2H, COCOHNCH_2), 4.5 (s, 2H, COHNCH_2), 5.21 (s, 2H, NCH_2), 7.01 (s, 2H, Ar-H), 7.16 (s, 2H, Ar-H), 7.30 (d, J = 6.35 Hz, 3H, Ar-H), 7.42 (d, J = 6.35, 3H, Ar-H), 7.85 (s, 2H, Ar-H), 7.91 (s, 2H, Ar-H), 8.01 (s, 1H, Ar-H), 9.13 (s, 1H, NH), 9.35 (s, 1H, NH) ppm; ^{13}C-NMR (75 MH_Z, DMSO-d6): δ 46.4, 47.5, 55.1, 126.3, 127.5, 128.8, 129.0, 131.3, 131.6, 134.1, 134.3, 134.5, 135.1, 135.4, 135.6, 136.3, 136.6, 140.3, 144.8, 145.1, 146.2, 168.0, 169.6, 170.3 ppm; IR (KBr): 3367, 3086, 2962, 1670, 1545 cm^{-1}.

N-(3-(Trifluoromethyl)benzyl)-3-(2-(3-(trifluoromethyl)benzylamino)-N-(4-(trifluoromethyl)benzyl)-2-oxoacetamido)benzamide (9i)

3-(Trifluoromethyl)phenyl)methanamine (**8c**, 0.155 ml, 1.37 mmol) together with 5 ml of TEA and 10 ml of DCM were added to **7c** (0.64 mmol), then the reaction mixture was stirred at room temperature for 5 days. Then the crude product was purified by column chromatography using chloroform: methanol, 98: 2 as eluent. Viscous compound was obtained **9i** (0.157 g, % yield = 23 %); $C_{33}H_{24}F_9N_3O_3$; R_f = 0.69 (chloroform: methanol, 98: 2), ^{1}H-NMR (500 MH_Z, DMSO-d6): δ 4.25 (d, J = 6.9 Hz, 2H, COCOHNCH_2), 4.57 (d, J = 6.75 Hz, 2H, COHNCH_2), 5.10 (s, 2H, NCH_2), 7.11 (s, 2H, Ar-H), 7.34-7.68 (m, 12H, Ar-H), 7.81 (s, 1H, Ar-H), 7.78 (s, 1H, Ar-H), 9.17 (t, J = 6.9 Hz, 1H, NH), 9.38 (t, J = 6.75 H_Z, 1H, NH) ppm; ^{13}C-NMR (100 MH_Z, DMSO-d6): δ 42.8, 43.9, 55.1, 124.0, 124.3, 125.8, 126.1, 129.1, 129.5, 129.7, 129.8, 131.6, 131.9, 140.1, 141.5, 165.3, 166.4, 169.5 ppm; IR (KBr): 3359, 3271, 3109, 2965, 1638,1576,1539 cm^{-1}.

N-(3,5-Bis(trifluoromethyl)benzyl)-3-(2-(3,5-bis(trifluoromethyl)benzylamino)-N-(4-(trifluoromethoxy)benzyl)-2-oxoacetamido)benzamide(9j)

(3,5-Bis(trifluoromethyl)phenyl)methanamine (**8d**, 0.155 ml, 1.37 mmol) together with 5 ml of TEA and 10 ml of DCM were added to **7a** (0.64 mmol), then the reaction mixture was stirred at room temperature for 5 days. Then the crude product was purified by column chromatography using chloroform: methanol, 98: 2 as eluent. Viscous compound was obtained **9j (**0.064 g, % yield = 12 %); $C_{35}H_{22}F_{15}N_3O_4$; R_f = 0.68 (chloroform: methanol, 98: 2), ^{1}H-NMR (500 MH_Z, DMSO-d6): δ 2.52 (s, 2H, COCOHNCH_2), 4.66 (d, J = 5.6 H_Z, 2H, COHNCH_2), 5.11 (s, 2H, NCH_2), 7.27 (d, J = 8.1 Hz, 2H, Ar-H), 7.36 (d, J = 8.2 Hz, 2H, Ar-H), 7.45 - 7.58 (m, 4H, Ar-H), 7.75 (d, J = 7.55 Hz, 1H, Ar-H), 7.85 (s, 1H, Ar-H), 8.01 (s, 4H, Ar-H), 8.74 (s, 1H, NH), 9.23 (t, J = 5.65 H_Z, 1H, NH) ppm; ^{13}C-NMR (125 MH_Z, DMSO-d6): δ 42.6, 46.4, 51.5, 119.5, 121.2, 121.5, 121.9, 122.7, 124.9, 125.4, 126.1, 128.7, 129.6, 130.2, 130.6, 130.8, 135.6, 136.7,141.2, 143.6, 147.8, 163.1, 163.7, 166.5 ppm; IR (KBr): 3260, 3304, 2932, 1702, 1645, 1588 cm^{-1}.

N-(3,5-Bis(trifluoromethyl)benzyl)-3-(N-(3,5-bis(trifluoromethyl)benzyl)-2-(3,5-bis(trifluoromethyl)benzylamino)-2-oxoacetamido)benzamide(9k)

(3,5-Bis(trifluoromethyl)phenyl)methanamine (**8d**, 0.155 ml, 1.37 mmol) together with 5 ml of TEA and 10 ml of DCM were added to **7b** (0.64 mmol), then the reaction mixture was stirred at room temperature for 5 days. Then the crude product was purified by column chromatography using chloroform: methanol, 98: 2 as eluent. Viscous compound was obtained **9k** (0.079 g, % yield = 14 %); $C_{36}H_{21}F_{18}N_3O_3$; R_f = 0.68 (chloroform: methanol, 98: 2), ^{1}H-NMR (500 MH_Z, DMSO-d6): δ 4.35 (s, 2H, COCOHNCH_2), 4.63 (d, J = 5.6 H_Z, 2H, COHNCH_2), 5.21 (s, 2H, NCH_2), 7.29 (s, 2H, Ar-H), 7.78-7.99 (m, 11H, Ar-H), 9.20 (t, J = 5.65 H_Z, 1H, NH), 9.52 (t, J = 5.65 H_Z, 1H, NH) ppm; ^{13}C-NMR (75 MH_Z, DMSO-d6): δ 41.5, 42.5, 50.9, 121.1, 121.1, 122.2, 123.6, 125.6, 126.4, 127.6, 128.5, 128.6, 128.8, 129.0, 130.5, 130.8, 131.5, 135.2, 143.4, 143.5, 164.1, 165.6 ppm; IR (KBr): 3380, 3255, 3093, 1657, 1587, 1546 cm^{-1}.

N-(3,5-Bis(trifluoromethyl)benzyl)-3-(2-(3,5-bis(trifluoromethyl)benzylamino)-N-(4-(trifluoromethyl)benzyl)-2-oxoacetamido)benzamide (9l)

(3,5-Bis(trifluoromethyl) phenyl)methanamine (**8d**, 0.155 ml, 1.37 mmol) together with 5 ml of TEA and 10 ml of DCM were added to **7c** (0.64 mmol), then the reaction mixture was stirred at room temperature for 5 days. Then the crude product was purified by column chromatography using chloroform: methanol, 98: 2 as eluent. Off white powder was obtained **9l** (0.105 g, % yield = 20 %); $C_{35}H_{22}F_{15}N_3O_3$; m.p =150° -151°; R_f = 0.64 (chloroform: methanol , 98: 2), ^{1}H-NMR (300 MH_Z, $CDCl_3$-d6): δ 4.55 (d, J = 4.41 Hz, 2H, COCOHNCH_2), 4.71 (s, 2H, COHNCH_2), 5.03 (s, 2H, NCH_2), 6.91 (d, J = 6.0 Hz, 2H, Ar-H), 7.35 (d, J = 6.24 Hz, 3H, Ar-H), 7.54-7.60 (m, 3H, Ar-H), 7.66 (s, 2H, Ar-H), 7.79-7.86 (m, 3H, Ar-H), 7.95 (s, 1H, Ar-H), 8.83 (s, 1H, NH) 10.0 (t, J = 5.65 H_Z, 1H, NH) ppm; ^{13}C-NMR (75 MH_Z, $CDCl_3$-d6): δ 43.1, 51.6, 54.8, 121.7, 122.5, 124.4, 125.4, 125.5, 125.7, 125.9, 126.3, 127.5, 127.9, 129.2, 129.9, 130.4, 131.9, 132.2, 134.0, 134.3, 139.6, 139.8, 139.9, 140.6, 140.7,160.1,

163.5, 165.9 ppm; IR (KBr): 3401, 3239, 3072, 2918, 1636, 1587, 1544 cm^{-1}.

N-(2-Methoxybenzyl)-3-(2-(2-methoxybenzylamino)-N-(4-(trifluoromethoxy)benzyl)-2-oxoacetamido)benzamide (9m)

(2-Methoxyphenyl)methanamine(**8e**, 0.155 ml, 1.37 mmol) together with 5 ml of TEA and 10 ml of DCM were added to **7a** (0.64 mmol), then the reaction mixture was stirred at room temperature for 5 days. Then the crude product was purified by column chromatography using chloroform: methanol, 98: 2 as eluent. White powder was obtained **9m** (0.044 g, % yield = 11 %); $C_{33}H_{30}F_3N_3O_6$; m.p = 190° -191°; R_f = 0.81 (chloroform: methanol, 98: 2), ^{1}H-NMR (500 MH_Z, DMSO-d6): δ 3.76 (s, 3H, OCH_3), 3.84 (s, 3H, OCH_3), 4.10 (d, *J* = 5.75 Hz, 2H, COCOHNCH_2), 4.46 (d, *J* = 5.55 H_Z, 2H, COHNCH_2), 5.04 (s, 2H, NCH_2), 6.73 (d, *J* = 7.40 Hz, 1H, Ar-*H*), 6.76 (t, *J* = 7.45 Hz, 1H, Ar-*H*), 6.88-6.93 (m, 2H, Ar-*H*), 7.00 (d, *J* = 8.20 Hz, 2H, Ar-*H*), 7.17 (d, *J* = 7.25 H_Z, 2H, Ar-*H*), 7.24 (t, *J* = 7.6 H_Z, 2H, Ar-*H*), 7.31 (t, *J* = 8.40 H_Z, 2H, Ar-*H*), 7.38-7.41 (m, 2H, Ar-*H*), 7.86-7.90 (m, 2H, Ar-*H*), 8.85 (t, *J* = 5.75 H_Z, 1H, N*H*), 9.06 (t, *J* = 5.70 H_Z, 1H, N*H*) ppm; ^{13}C-NMR (125 MH_Z, DMSO-d6): δ 37.1, 38.2, 55.7, 110.8, 110.9, 119.5, 120.5, 121.4, 121.5, 125.9, 126.7, 126.8, 127.1, 127.7, 127.9, 128.5, 129.5, 130.3, 130.6, 135.8, 136.5, 140.9, 148.0, 156.8, 157.1, 163.6, 165.6, 165.7 ppm; IR (KBr): 3402, 3287, 2964, 2842, 1676, 1662, 1493 cm^{-1}.

N-(2-Methoxybenzyl)-3-(2-(2-methoxybenzylamino)-N-(3,5-bis(trifluoromethyl)benzyl)-2-oxoacetamido)benzamide (9n)

(2-Methoxyphenyl)methanamine (**8e**, 0.155 ml, 1.37 mmol) together with 5 ml of TEA and 10 ml of DCM were added to **7b** (0.64 mmol), then the reaction mixture was stirred at room temperature for 5 days. Then the crude product was purified by column chromatography using chloroform: methanol, 98: 2 as eluent. White powder was obtained **9n** (0.159 g, % yield = 37 %); $C_{34}H_{29}F_6N_3O_5$; m.p = 110°-111°; R_f = 0.73 (chloroform: methanol, 98: 2), ^{1}H-NMR (300 MH_Z, DMSO-d6): δ 3.74 (s, 3H, OCH_3), 3.81 (s, 3H, OCH_3), 4.09 (s, 2H, COCOHNCH_2), 4.44 (s, 2H, COHNCH_2), 5.19 (s, 2H, NCH_2), 6.59 (s, 1H, Ar-*H*), 6.71 (s, 1H, Ar-*H*), 6.87-6.99 (m, 3H, Ar-*H*), 7.13-7.23 (m, 3H, Ar-*H*),), 7.32-7.38 (m, 2H, Ar-*H*), 7.86-8.02 (m, 5H, Ar-*H*), 8.86 (t, *J* = 5.78 H_Z, 1H, N*H*), 9.12 (t, *J* = 5.73 H_Z, 1H, N*H*) ppm; ^{13}C-NMR (75 MH_Z, DMSO-d6): δ 38.1, 39.5, 50.7, 55.7, 110.8, 110.9, 120.4, 120.5, 122.6, 125.8, 126.6, 126.9, 127.0, 127.7, 127.8, 128.5, 128.6, 129.3, 129.6, 130.4, 130.9, 135.9, 135.9, 140.5, 140.6, 156.8, 157.0, 163.4, 165.6, 165.8 ppm; IR (KBr): 3389, 3257, 2964, 2838, 1704, 1688, 1495 cm^{-1}.

N-(2-Methoxybenzyl)-3-(2-(2-methoxybenzylamino)-N-(4-(trifluoromethyl)benzyl)-2-oxoacetamido)benzamide (9o)

(2-Methoxyphenyl)methanamine (**8e**, 0.155 ml, 1.37 mmol) together with 5 ml of TEA and 10 ml of DCM were added to **7c** (0.64 mmol), then the reaction mixture was stirred at room temperature for 5 days. Then the crude product was purified by column chromatography using chloroform: methanol, 98: 2 as eluent. Off white powder was obtained **9o** (0.116 g, % yield = 30 %); $C_{33}H_{30}F_3N_3O_5$; m.p = 85° -86°; R_f = 0.73 (chloroform: methanol , 98: 2), ^{1}H-NMR (300 MH_Z, DMSO-d6): δ 3.86 (s, 3H, OCH_3), 3.90 (s, 3H, OCH_3), 4.59 (d, *J* = 4.38 Hz, 2H, COCOHNCH_2), 4.63 (d, *J* = 4.32 Hz, 2H, COHNCH_2), 4.98 (s, 2H, NCH_2), 6.84- 6.98 (m, 4H, Ar-*H*), 7.03 (d, *J* = 6.27 Hz, 1H, Ar-*H*), 7.12 (d, *J* = 5.43 Hz, 1H, Ar-*H*), 7.21-7.46 (m, 6H, Ar-*H*), 7.53-7.62 (m, 4H, Ar-*H*), 8.86 (t, *J* = 4.38 H_Z, 1H, N*H*), 9.12 (t, *J* = 4.32 H_Z, 1H, N*H*) ppm; ^{13}C-NMR (75 MH_Z, DMSO-d6): δ 34.6, 34.9, 49.6, 50.7, 105.6, 116.0, 120.4, 120.5, 122.6, 125.8, 126.6, 126.9, 127.0, 127.7, 127.8, 128.5, 128.6, 129.3, 129.6, 130.4, 130.9, 135.9, 135.9, 140.5, 140.6, 156.8, 157.0, 163.4, 165.6, 165.7 ppm; IR (KBr): 3367, 3244, 3078, 2930, 1669, 1544, 1444 cm^{-1}.

N-(2-(Trifluoromethyl)benzyl)-3-(2-(2-(trifluoromethyl)benzylamino)-N-(4-(trifluoromethoxy)benzyl)-2-oxoacetamido)benzamide (9p)

(2-(Trifluoromethyl)phenyl)methanamine (**8f**, 0.155 ml, 1.37 mmol) together with 5 ml of triethylamine and 10 ml of dichloromethane were added to **7a** (0.64 mmol), then the reaction mixture was stirred at room temperature for 5 days. Then the crude product was purified by column chromatography using chloroform: methanol, 98: 2 as eluent. Off white powder was obtained **9p** (0.126 g, % yield = 28.3 %); $C_{33}H_{24}F_9N_3O_4$; m.p = 130° -131°; R_f = 0.65 (chloroform: methanol, 98: 2), ^{1}H-NMR (500 MH_Z, DMSO-d6): δ 4.34 (d, *J* = 4.75 Hz, 2H, COCOHNCH_2), 4.68 (d, *J* = 4.70 H_Z, 2H, COHNCH_2), 5.07 (s, 2H, NCH_2), 6.88 (d, *J* = 7.25 Hz, 1H, Ar-*H*), 7.34 (d, *J* = 8.0 Hz, 2H, Ar-*H*), 7.41-7.51 (m, 7H, Ar-*H*), 7.61-7.68 (m, 3H, Ar-*H*), 7.76 (d, *J* = 7.65 Hz, 1H, Ar-*H*), 7.92 (d, *J* = 1.75 H_Z, 2H, Ar-*H*), 9.15 (t, *J* = 5.55 H_Z, 1H, N*H*), 9.39 (t, *J* = 4.70 H_Z, 1H, N*H*) ppm; ^{13}C-NMR (125 MH_Z, DMSO-d6): δ 38.6, 39.6, 51.2, 119.5, 121.5, 123.7, 123.9, 126.1, 126.3, 126.4, 126.8, 126.9, 127.0, 127.8, 128.6, 128.8, 129.3, 129.7, 130.3, 133.0, 135.4, 136.3, 137.9, 140.9, 148.1, 163.8, 165.2, 165.9 ppm; IR (KBr): 3353, 3214, 3072, 1695, 1652, 1584 cm^{-1}.

N-(2-(Trifluoromethyl)benzyl)-3-(2-(2-(trifluoromethyl)benzylamino)-N-(3,5-bis(trifluoromethyl)benzyl)-2-oxoacetamido)benzamide (9q)

(2-(Trifluoromethyl)phenyl)methanamine (**8f**, 0.155 ml, 1.37 mmol) together with 5 ml of triethylamine and 10 ml of dichloromethane were added to **7b** (0.64 mmol), then the reaction mixture was stirred at room temperature for 5 days. Then the crude product was purified by column chromatography using chloroform: methanol, 98: 2 as eluent. Viscous compound obtained **9q** (0.083 g, % yield = 20 %); $C_{34}H_{23}F_{12}N_3O_3$; R_f = 0.7 (chloroform: methanol, 98: 2), ^{1}H-NMR (300 MH_Z, DMSO-d6): δ 4.31 (s, 2H, COCOHNCH_2), 4.63 (s, 2H, COHNCH_2), 5.20 (s, 2H, NCH_2), 6.84 (d, *J* = 5.04 Hz, 1H, Ar-*H*), 7.36-7.47 (m, 6H, Ar-*H*), 7.55-7.63 (m, 2H, Ar-*H*), 7.71 (d, *J* = 5.73 Hz, 2H, Ar-*H*), 7.87 (d, *J* = 9.12 Hz, 4H, Ar-*H*) 8.00 (s, 1H, Ar-*H*), 9.11 (s, 1H, N*H*), 9.39 (s, 1H, N*H*) ppm; ^{13}C-NMR (75 MH_Z, DMSO-d6): δ 39.3, 45.6, 55.1, 116.5, 117.1, 117.5, 118.2, 119.7, 121.0, 121.5, 121.8, 122.6, 123.3, 123.5, 124.1, 124.5, 125.4, 125.7, 127.7, 130.5, 131.3, 132.5, 135.1, 135.4, 158.2, 160.1, 160.5 ppm; IR (KBr): 3411, 3246, 3065, 2963, 1694, 1642, 1586 cm^{-1}.

N-(2-(Trifluoromethyl)benzyl)-3-(2-(2-(trifluoromethyl)benzylamino)-N-(4-(trifluoromethyl)benzyl)-2-oxoacetamido)benzamide (9r)

(2-(Trifluoromethyl)phenyl)methanamine (**8f**, 0.155 ml, 1.37 mmol) together with 5 ml of triethylamine and 10 ml of dichloromethane were added to **7c** (0.64 mmol), then the reaction mixture was stirred at room temperature for 5 days. Then the crude product was purified by column chromatography using chloroform: methanol, 98: 2 as eluent. Off white powder

was obtained **9r** (0.113 g, % yield = 26 %); $C_{33}H_{24}F_9N_3O_3$; m.p = 115°-116°; R_f = 0.72 (chloroform: methanol, 98: 2), ^{1}H-NMR (300 MH_Z, $CDCl_3$-d6): δ 4.52 (d, *J* = 4.59 Hz, 2H, COCOHNCH_2), 4.80 (d, *J* = 4.44 H_Z, 2H, COHNCH_2), 4.99 (s, 2H, NCH_2), 7.09 (d, *J* = 5.79 Hz, 1H, Ar-*H*), 7.33-7.44 (m, 6H, Ar-*H*), 7.47 (d, *J* = 6.51 H_Z, 2H, Ar-*H*), 7.55 (d, *J* = 5.73 H_Z, 4H, Ar-*H*), 7.63-7.68 (m, 2H, Ar-*H*), 7.70 (d, *J* = 5.88 H_Z, 1H, Ar-*H*), 8.90 (t, *J* = 4.59 H_Z, 1H, N*H*), 9.16 (t, *J* = 4.44 H_Z, 1H, N*H*) ppm; ^{13}C-NMR (75 MH_Z, $CDCl_3$-d6): δ 40.0, 40.3, 54.4, 122.6, 122.9, 123.1, 125.3, 125.6, 125.7, 125.9, 126.1, 126.2, 127.9, 128.4, 128.6, 129.0, 129.5, 130.0, 130.1, 130.5, 131.2, 132.4, 135.2, 135.5, 136.2, 139.2, 142.2, 159.7, 162.0, 166.0 ppm; IR (KBr): 3362, 3277, 3071, 2961, 1680, 1657, 1586 cm^{-1}.

Anti-CETP Assay

The synthesized compounds **9a**-**r** were evaluated for their anti-CETP using a purchased kit (MyBiosource CETP Inhibitor Screening Kit (Fluorometric), USA) [22]. Briefly, the kit encompasses human CETP, donor and acceptor molecules. When the CETP transfers the fluorescent fat from the donor to the acceptor molecule the fluorescence rises. Inhibition of CETP results in reduced fluorescence. 2 µL of the inhibitor was mixed with 5 µL of CETP, then a 5 µL of each donor and acceptor molecules were added and the volume was continued to 200 µL using the buffer solution. Afterward, the mixture was incubated at 37°C for 30 minutes, then the fluorescent intensity was measured with FLX800TBI Microplate Fluorimeter (BioTek, Winooski, VT, USA) at wavelength of 511 nm for emission and 480 nm for excitation.

The inhibitors were evaluated for CETP inhibitory activity at a concentration of 10 µM, in addition to reading blanks. Negative control that lacks CETP was tested, and the CETP inhibitor Anacetrapib was used as a positive reference. Test was carried out in duplicates. Using the following equation, the percentage of CETP inhibition was calculated:

Inhibition percentage = [1-(Inhibitor read-Blank read)/ (Positive control-Negative control)]*100%

For IC_{50} determination, the inhibitors' activity was evaluated at three different concentrations (10, 1.0, and 0.1 µM) followed by plotting the % of CETP inhibition versus log concentration, and the best fit line was drawn. From the equation of that dose-response line, the IC_{50} values were calculated.

In Silico Studies

Preparation of Synthesized Compounds and Protein Structure

The crystal assembles of cholesteryl ester transfer protein (CETP) (PDB ID: 4EWS) [25] was fetched from the RCSB Protein Data Bank. Ensembles of 4EWS was selected because it's a human-derived structure embedding a ligand and its resolution (2.59 Å) surpasses the other structures. CETP structure was treated and energetically decreased using the Protein Preparation [26] algorithm in Schrödinger program to enhance H-bond linkage. Protein preparation module in MAESTRO [26] was employed to assign bond order, add Hydrogens (H), create zero-order bonds to metals, create disulfide bonds, convert selenomethionines to methionines, fill up the missing sequences, cap the *N*-and *C*-termini, minimize H atoms, and optimize protein's H-bond organization, delete waters beyond 5 Å, and generate het states using Epk: pH 7±2. Then, the protein was refined and optimized for H-bond assignment. This assignment is an automated process in which all H-bonds were optimized. Additionally, an interactive optimization in which various clusters of H-bonded species can be effectively optimized. Further protein refinement was carried out by minimizing the protein side chain while constraining the protein backbone amino acids using optimized potentials for liquid simulations-2005 (OPLS_2005) force field. Next, the proteins' side chains were further energetically minimized to reduce steric clashes. The protein preparation protocol is a proceeding step for docking using MAESTRO in SCHRODINGER Enterprise. If the protein structure isn't well-prepared, minimized, and optimized, the docking protocol will not work.

The tested compounds (ligands) were depicted using the coordinates of the co-ligand (0RP) in the crystal structure of 4EWS [25]. Ligands were patterned by MAESTRO build wizard and energetically prepared by MacroModel [26] algorithm by OPLS2005 force field. All small-molecule chemical structures were prepared as the following: 1) generate 3D coordinates of all potential ligands based on the template of the co-crystallized ligand (ORP) in 4EWS using "Build" wizard in MAESTRO [26], 2) the 3D ligand coordinates were energetically treated using the "ligprep" script in MAESTRO [26]. LigPrep probed stereoisomerism, tautomerism, ring conformations, and ionization state. LigPrep generated diverse chemical and structural features from a single structure.

Induced-fit docking (IFD)

The co-ligand (0RP) was designated as a centroid in 4EWS binding site. The Vander Waals' measuring factors for CETP and ligand were mounted to 0.5 to provide sufficient pliability for the upmost docked ligand pose. Extra IFD preferences were scaled as default. The ligand's geometry with the high XP Glide score was recorded as recommended by SCHRODINGER developers. The binding energy represents the docking score (kcal/mol). The more negative docking score defines favored binding interaction. IFD treats the protein side chain as a relaxed ensemble by minimizing the side chain of the protein prior docking and implements molecular mechanics (MM) tools.

The binding site surrounds the co-crystallized ligand. The docking algorithm in MAESTRO assigns the co-ligand and automatically calculates the binding site dimensions based on three axis (x, y, and z). If there is an allosteric binding site provided having a co-ligand, the same procedure is applied. The binding site dimensions could be modified based on the researcher's willing. Actually, the docking algorithm is easily going calculations provided the perquisite protein and ligand preparations are properly accomplished. The binding affinity values for the same set of ligands can be compared, if the protein structure has an active and allosteric domains to confirm the findings. Besides, the superposing of the docked pose of the co-crystallized ligand to its native geometry validates the results and define the reliability of the docking protocol.

Prime MMGBSA

The binding free energy of CETP receptor and ligand complex was calculated using Prime MMGBSA (Molecular Mechanics Generalized Born Surface Area) script in Schrodinger enterprise with the OPLS_2005 force field [26]. The binding free energy of a ligand (L) to a receptor (R) to form the complex (RL) is expressed by the attached equation:

ΔGbinding = ΔG (*complex*)-ΔG (*Receptor*)-ΔG (*Ligand*)

G Binding is the binding free energy; while G complex, G receptor and G ligand represent the free energy of complex, receptor, ligand, respectively.

intermediates (**5a-c**). Dichloromethane (DCM) was the used solvent, whereas triethylamine (TEA) was used as an acid

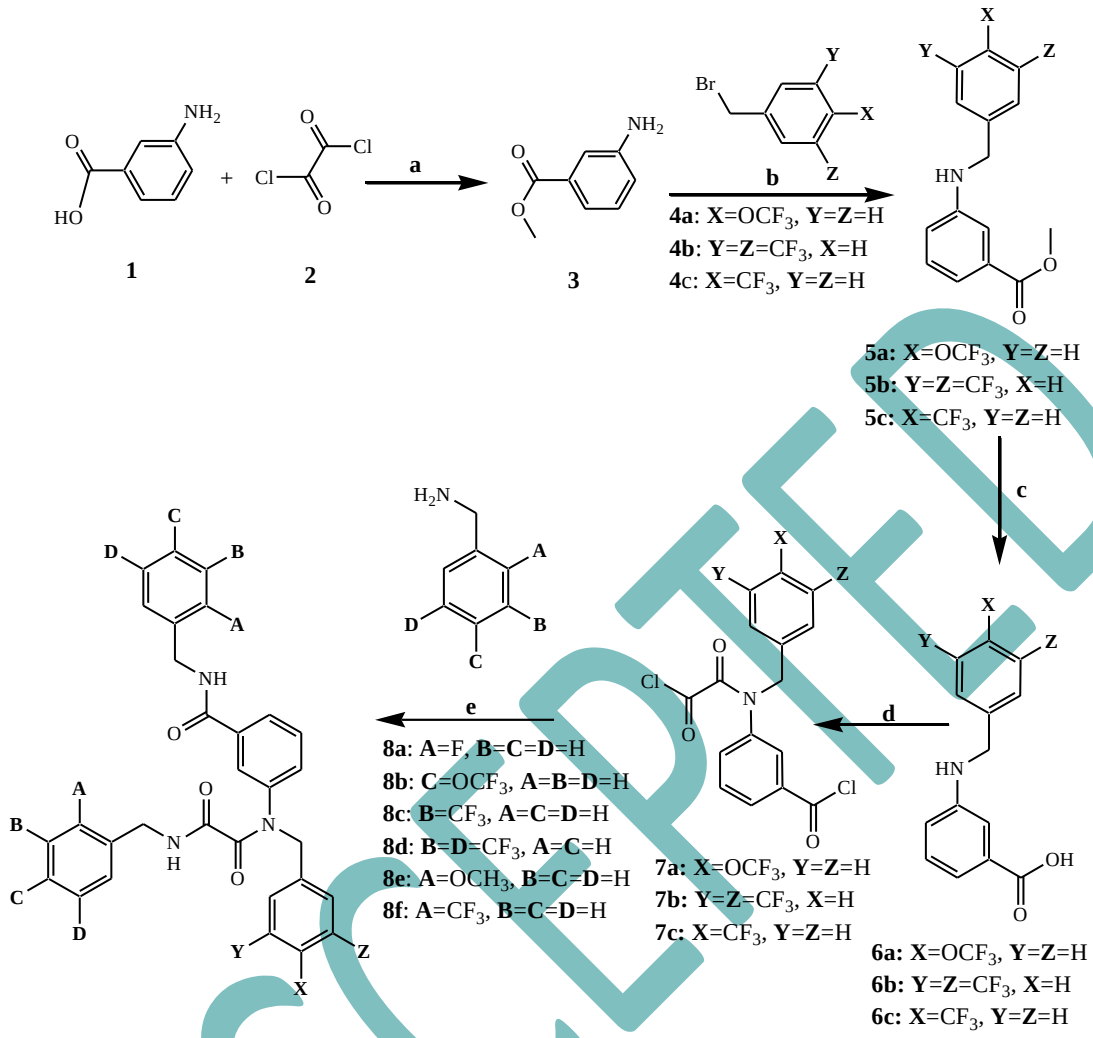

9a: **X**=OCF_3, **Y**=**Z**=H, **A**=F, **B**=**C**=**D**=H
9b: **Y**=**Z**=CF_3, **X**=H, **A**=F, **B**=**C**=**D**=H
9c: **X**=CF_3, **Y**=**Z**=H, **A**=F, **B**=**C**=**D**=H
9d: **X**=OCF_3, **Y**=**Z**=H, **C**=OCF_3, **A**=**B**=**D**=H
9e: **Y**=**Z**=CF_3, **X**=H, **C**=OCF_3, **A**=**B**=**D**=H
9f: **X**=CF_3, **Y**=**Z**=H, **C**=OCF_3, **A**=**B**=**D**=H
9g: **X**=OCF_3, **Y**=**Z**=H, **B**=CF_3, **A**=**C**=**D**=H
9h: **Y**=**Z**=CF_3, **X**=H, **B**=CF_3, **A**=**C**=**D**=H
9i: **X**=CF_3, **Y**=**Z**=H, **B**=CF_3, **A**=**C**=**D**=H
9j: **X**=OCF_3, **Y**=**Z**=H, **B**=**D**=CF_3, **A**=**C**=H
9k: **Y**=**Z**=CF_3, **X**=H, **B**=**D**=CF_3, **A**=**C**=H
9l: **X**=CF_3, **Y**=**Z**=H, **B**=**D**=CF_3, **A**=**C**=H
9m: **X**=OCF_3, **Y**=**Z**=H, **A**=OCH_3, **B**=**C**=**D**=H
9n: **Y**=**Z**=CF_3, **X**=H, **A**=OCH_3, **B**=**C**=**D**=H
9o: **X**=CF_3, **Y**=**Z**=H, **A**=OCH_3, **B**=**C**=**D**=H
9p: **X**=OCF_3, **Y**=**Z**=H, **A**=CF_3, **B**=**C**=**D**=H
9q: **Y**=**Z**=CF_3, **X**=H, **A**=CF_3, **B**=**C**=**D**=H
9r: **X**=CF_3, **Y**=**Z**=H, **A**=CF_3, **B**=**C**=**D**=H

Scheme (1): Synthesis of compounds **9a**-**r**. Reagents and conditions: (**a**) CH_3OH/reflux (60-70°C), 24 hrs, (**b**) DCM, TEA, rt, 5 days, (**c**) (**1**) 1M NaOH (100°C), overnight, (**2**) Conc. HCl, (**d**) $(COCl)_2$ /reflux (60-70°C), DCM, 4 days, (**e**) TEA, DCM, rt, 5 days.

Results and Discussion

Chemistry

Scheme **1** shows the preparation of eighteen derivatives of benzyl benzamides **9a**–**r**. The preparation steps from **1** to **5** were carried out as reported earlier [18-20]. Briefly, esterification of 3-aminobenzoic acid (**1**) was achieved by refluxing it with methanol after its carboxyl group was activated using oxalyl chloride (**2**).

Then, nucleophilic addition-elimination reaction took place by the attack from the amine group of the formed ester **3** on the methylene carbon atom of benzyl bromide (**4a-c**) to produce scavenger.

Afterward, the carboxylic acid group of 3-aminobenzoic acid methyl ester intermediates **5a**, **5b**, and **5c** was deprotected using 1M NaOH under reflux followed by neutralization with 1 M HCl. Then, the carboxylic acid moiety of 3-benzylamino benzoic acid intermediates **6a**, **6b**, and **6c** was activated using oxalyl chloride (**2**) in the presence of TEA and DCM to produce the corresponding acyl chloride derivatives.

Moreover, -NH_2 moiety of intermediates **6a**, **6b**, and **6c** reacted with oxalyl chloride. Subsequently, amide formation was attained by the nucleophilic attack of -NH_2 moiety of benzylamine

8a–f on the partially positive carbonyl carbon of the previously produced benzoyl chloride and acyl chloride to form the desired products **9a–r**. The best yield was obtained upon reacting intermediate **7c** with 2-fluorobenzylamine (**8a**) to produce **9c** in 52.5% yield.

Anti-CETP Assay

Table **1** demonstrated that most of the synthesized compounds have a significant activity against CETP at a concentration of 10 µM. So, the inhibitory activity of these compounds was evaluated at lower concentrations (1.0 and 0.1 µM), and their IC_{50} values were determined (Table **1**).

The *in vitro* biological data declare that compounds **9g**, **9h**, **9l**, and **9r** exhibited the highest CETP inhibitory activity (represents in IC_{50} value) inferring the importance of substitution pattern on aromatic rings. Remarkably, tailoring two aromatic rings with *m*-CF_3 and another aromatic ring with *p*-CF_3 (**9l**) induces the activity implying the significance of hydrophobic motif that accor1ds with the hydrophobic residues in the binding domain. Interestingly, incorporating of *m*-CF_3 on two aromatic rings and 3,5-bis-CF_3 on a third ring (**9h**) provokes the activity. Furthermore, attaching of *m*-CF_3 on two aromatic rings and one *m*-CF_3 on a third ring (**9r**) induces the activity.

Table (1): CETP inhibitory results of the synthesized benzamides **9a**-**r**.

Compound	% of CETP Inhibition (at 10.0 µM) ± SD	IC_{50} (µM)
9a	85.2 ± 0.5	1.24
9b	81.0 ± 0.4	1.00×10^{-1}
9c	81.7 ± 0.8	1.50×10^{-4}
9d	83.2 ± 0.3	1.10×10^{-1}
9e	87.8 ± 0.4	4.60×10^{-1}
9f	72.8 ± 0.6	1.00×10^{-3}
9g	93.0 ± 0.5	1.03×10^{-6}
9h	100.0 ± 0.7	6.54×10^{-6}
9i	100.0 ± 0.6	1.70×10^{-1}
9j	85.0 ± 0.2	1.00×10^{-2}
9k	99.3 ± 0.6	7.05×10^{-4}
9l	100.0 ± 0.8	7.16×10^{-8}
9m	78.7 ± 0.3	8.20×10^{-3}
9n	87.6 ± 0.7	4.80×10^{-1}
9o	81.3 ± 0.4	4.00×10^{-2}
9p	85.3 ± 0.4	5.60×10^{-3}
9q	97.8 ± 0.8	1.80×10^{-3}
9r	100.0 ± 0.4	9.03×10^{-7}
Anacetrapib	60.5* ± 0.6	5.00×10^{-3}

SD: Standard deviation, *: at concentration of 0.08 µM.

Notably, introducing *p*-CF_3 on two aromatic rings and *p*-OCF_3 on the third ring (**9g**) suggesting that *m*-or *p*-CF_3 on two aromatic rings are recommended to incite the activity. Moreover, the importance of *p*-OCF_3 on the third ring is comparable to that of *p*-CF_3 indicating that a hydrophobic contour surrounding the *p*-position. However, tailoring three aromatic rings with 3,5-bis-CF_3 (**9k**) potentiates the activity inferring the worthiness of the number of hydrophobic groups, appropriate positions, and corresponding steric effect. Incorporating of *o*-F on two aromatic rings and *p*-CF_3 on a third ring (**9c**) and attaching of *p*-OCF_3 on two aromatic rings and *p*-CF_3 on a third ring (**9f**) increases the activity but not to the same extent of those of **9h**, **9l**, and **9r**. Harmoniously, attaching of *m*-CF_3 on two aromatic rings and 3,5-bis-CF_3 on a third ring (**9q**), incorporating two *o*-OCF_3 on two aromatic rings and the third ring unsubstituted (**9p**), and introducing two *o*-CH_3 on two aromatic rings and *p*-OCF_3 on a third ring (**9m**) increases the activity but not to the same extent of those of **9h**, **9l**, and **9r**.

Collectively, introducing two *o*-CH_3 on two aromatic rings and 3,5-bis-CF_3 on a third ring (**9n**), incorporating two *o*-CH_3 on two aromatic rings and *p*-CF_3 on a third ring (**9o**), and tailoring two aromatic rings with *p*-OCF_3 and a third ring with 3,5-bis-CF_3 (**9e**) vitalize the activity but not comparable to those of **9h**, **9l**, and **9r**. Attaching two *m*-CF_3 on two aromatic rings and *p*-CF_3 on a third ring (**9i**) and introducing two *m*-CF_3 on two aromatic rings and *p*-OCF_3 on a third ring (**9j**) inspires the activity but not comparable to those of **9h**, **9l**, and **9r**. Similarly, tailoring two aromatic rings with *o*-F and a third ring with 3,5-bis-CF_3 (**9b**) ignites the activity whereas introducing two aromatic rings with *o*-F and a third ring with two *p*-OCF_3 (**9a**) enhances the activity but not the same range of those of **9h**, **9l**, and **9r**. Furthermore, tailoring three aromatic ring with *p*-OCF_3 (**9d**) arouses the activity interrogating that hydrophobic force mediates inhibitor/CETP interaction.

From the above analysis of the bioassay data, the concluded structure-activity relationship is that regarding the **XYZ**-substituted aromatic ring, the presence of *p*-CF_3 group (**X**=CF_3) offered the optimum CETP inhibition as seen in compounds **9l** and **9r**. While, the presence of *p*-OCF_3 group (**X**=OCF_3) or 3,5-bis-CF_3 (**Y**=**Z**=CF_3) provided comparable less inhibitory activities as perceived in compounds **9g** and **9h**, respectively. On the other hand, concerning the **ABCD**-substituted aromatic ring, the presence of 3-CF_3 group (**B**=CF_3) as in inhibitors **9g** and **9h,** 2-CF_3 group (**A**=CF_3) as in inhibitor **9r**, and 3,5-bis-CF_3 (**B**=**D**=CF_3) as in **9l** offered the optimum CETP inhibition. Whereas, substitutions like 2-F, 2-OCH_3, and 4-OCF_3 (**A**=F, **A**=OCH_3, and **C**=OCF_3, respectively) presented relatively less active derivatives as in compounds **9a**, **9d**, **9b**, **9e**, **9n**, and **9o**.

In Silico Studies Results

In order to assess the manipulation of IFD program, we matched the docked pose of 0RP in CETP (PDB ID: 4EWS [25]) to its native template in the crystal assembly. Figure **2** demonstrates the superimposing of the IF-derived 0RP and its original conformation in 4EWS. The RMSD for heavy atoms of 0RP between IF-extracted docked pose and the native pose was 1.443 Å. Result implies that IFD can generate the original geometry in crystal trajectories and identify the conformation of inhibitor binding.

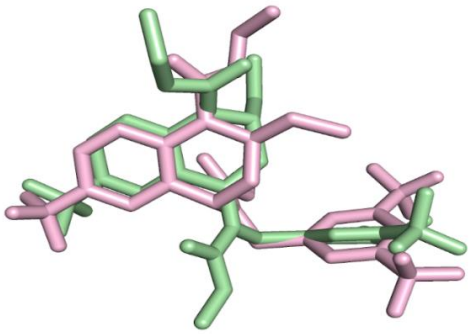

Figure (2): The superposing of the IF-docked 0RP pose (pink color) and its native trajectory (green color) in 4EWS. Picture portrayed by PYMOL.

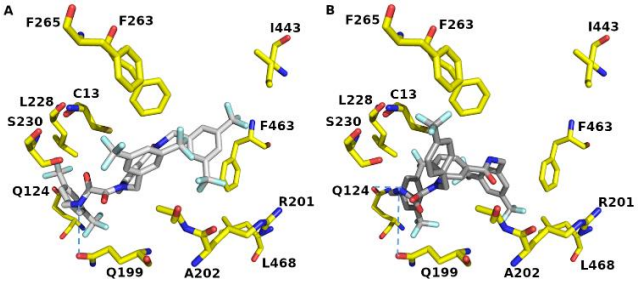

Figure (4): The IF docked conformations of (**A**) **9k**, and (**B**) **9l** in 4EWS binding site. H-Bond is pictured in blue dotted line. Picture portrayed by PYMOL.

Table (2): The IFD scores (kcal/mol), H-bonding, and MMGBSA ΔGbinding (kcal/mol).

Cpd	IFD scores	H-Bond	π–π stacking	MMGBSA ΔGbinding	Cpd	IFD scores	H-Bond	MMGBSA ΔGbinding
9a	-13.33	Q199	F263, F265	84.6	**9k**	-14.09	Q199	-110.3
9b	-13.11	NA	F263	-89.1	**9l**	-15.06	Q199, S230	-97.3
9c	-11.94	R201		-83.1	**9m**	-12.61	C13, S230	-91.8
9d	-11.05	NA		-105.5	**9n**	-11.91	NA	-99.5
9e	-13.07	R201, H232		-108.8	**9o**	-12.23	R201	-93.7
9f	-11.78	NA	H232	-95.1	**9p**	-12.33	Q199	-96.9
9g	-11.29	NA		-79.4	**9q**	-11.72	C13	-87.6
9h	-11.82	NA		-96.7	**9r**	-13.39	Q199, R201	-91.9
9i	-12.35	C13, S230	F265	-101.1	Torcetrapib	-9.57	R201	NA
9j	-13.52	NA	F263, F441, F461	-89.7	Anacetrapib	-11.69	Q199	-90.1

NA: Not available.

In order to explain the structural-basis of binding of anacetrapib, co-ligand (0RP: torcetrapib), and **9a**-**r**, we executed induced-fit docking (IFD) studies [26-28] against the coordinates of CETP (PDB ID: 4EWS) binding domain [25]. The IFD results illustrate that 0RP, anacetrapib, and **9a-r** accommodate 4EWS binding cleft (Figure **3**).

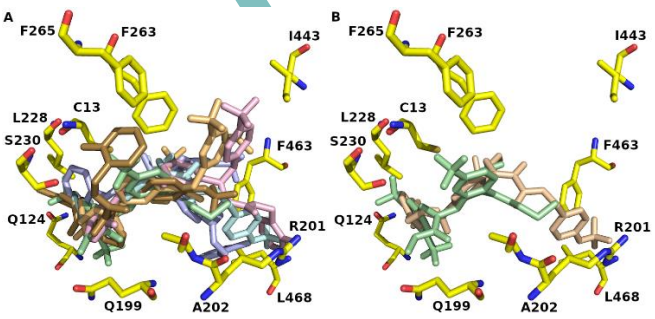

Figure (3): (**A**) 4EWS binding domain harboring the IF-docked poses of **9a**-**e**, and (**B**) Superimposing of the IFD geometry of **9d** (sand) and 0RP (green color). Picture portrayed by PYMOL.

The IFD data inform that hydrophobic force predominates inhibitor/CETP complex formation (Figures **4**-**6**) (Supplementary Figures **1S**-**7S**).

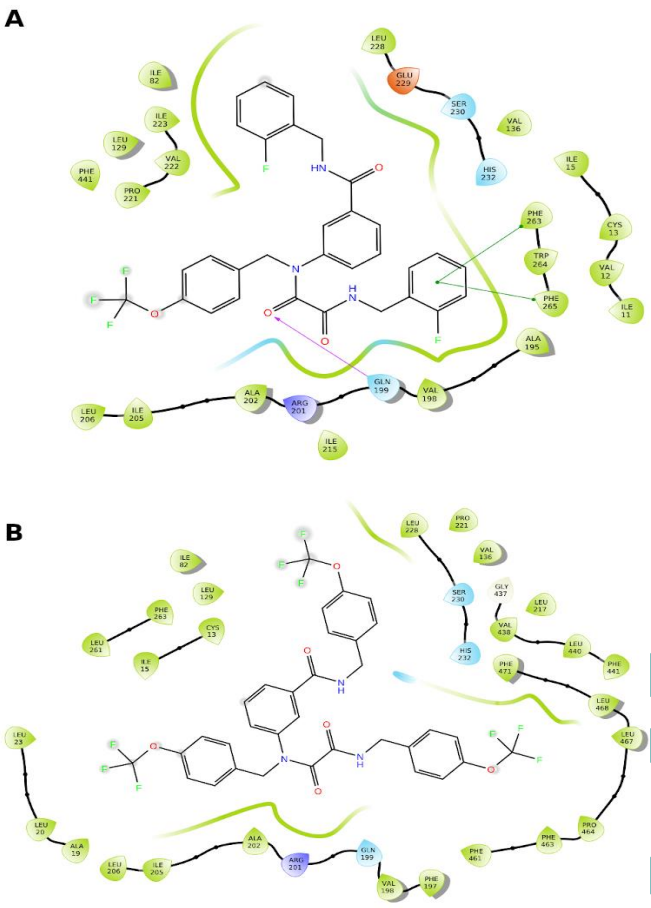

Figure (5): The inhibitor/CETP complex of (**A**) **9a**, and (**B**) **9d**. The hydrophobic curve is green colored. Picture portrayed by MAESTRO [26].

The hydrophobic interaction is extrapolated from the nearby residues surrounding the ligand. The mode of interaction is like dissolve like and this supports that hydrophobic ligand is surrounded by hydrophobic residues. By inspecting the aromatic and hydrophobic binding residues (green color) that are spread over the binding domain, it was found that the binding domain encloses I11, V12, I15, I82, L129, V136, A195, V198, A202, I205, L206, I215, V222, I223, L228, F263, W264, F265, F441, I443, F463, and L468. Such residues are aromatic and hydrophobic. And, the ligand interaction tool in SCHRODINGER highlight such residues by green contour as globally agreed and is described as greasy i.e. due to its lipophilic characteristic.

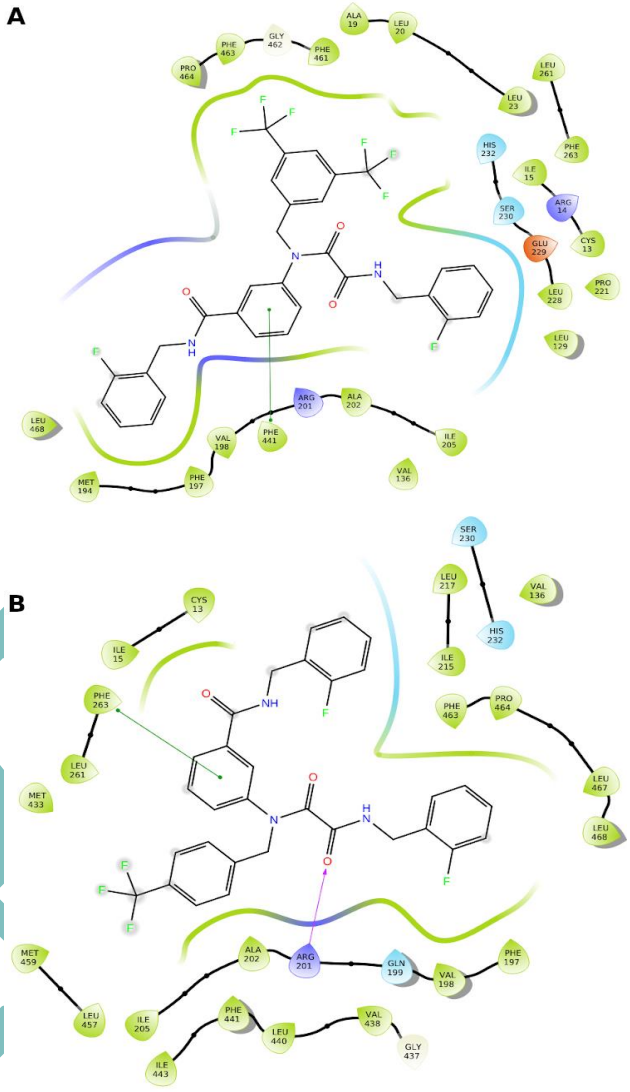

Figure (6): The inhibitor/CETP complex of (**A**) **9b**, and (**B**) **9c**. The hydrophobic curve is green colored. Picture portrayed by MAESTRO [26].

The hydrophobic contour surrounds the backbone of all ligands interrogating that hydrophobic interaction drives ligand/receptor complex formation as shown in Figures **5** and **6** and Supplementary Figures **1S** -**3S** beside the aromatic-aromatic interaction (π–π stacking) for compounds (**9a**, **9b**, **9f**, **9i**, and **9j**) as seen in Table **2**. Compounds bind with C13, Q199, R201, and H232 through H-bond (Table **2**). Further docking studies reported the prevalence of these residues in inhibitor/CETP interaction [19, 22]. Interestingly, the core structure of this scaffold is rigid due to the presence of four aromatic rings and incorporation of one and/or two carbonyl motif (s) in the side chain; both features decrease the number of generated conformations in the binding domain and consequently increase the binding affinity.

The reported Prime MMGBSA results estimate the binding free energy more accurately than docking scores and are valuable for indicating the strength and stability of binding interactions, disclosing binding free energies (ΔG), ranging between -79.4 to -110.3 (kcal/mol). The more the negative the ΔG, the more stable (LR) complex [29, 30]. Indeed, the ΔG of the

verified analogues surpass that of co-crystallized ligand (0RP) and the reference inhibitor (Anacetrapib) anticipating the matching of analogues' core structures to CETP key binding residues.

In order to explore the scaffold's core nucleus and attached groups, we screened the series against a recorded pharmacophore model of active CETP inhibitors [19]. Results demonstrate that the verified derivatives validate the fingerprint of CETP active inhibitors (Figure **7**) and subsequently elaborate the binding score values against CETP binding domain. Remarkably, the harboring of analogues in CETP binding site interprets their potential inhibitory activity.

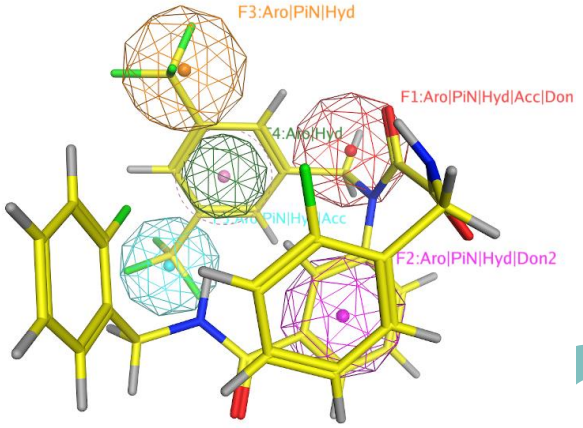

Figure (7): Pharmacophore model of CETP active inhibitor with **9b**. Acc represents H-bond acceptor; Aro aromatic ring; Cat cationic group; Don H-bond donor; Hyd hydrophobic group; and PiN π-ring. Picture portrayed by MOE [31].

Conclusion

Successful synthesis, characterization, and *in vitro* study for eighteen new trifluoro-oxoacetamido benzamides **9a-r** were carried out. *In vitro* study showed that the targeted compounds **9a-r** exhibit distinguished activity against CETP, where compound **9l** has an IC_{50} of 7.16×10^{-8} µM. Induced-fit docking results illustrate that the target compounds **9a-r** accommodate CETP binding cleft and that hydrophobic interaction predominates inhibitor/CETP complex formation. Compounds **9a-r** confirm the fingerprint of CETP active inhibitors and subsequently elaborate the binding score values against CETP binding domain.

Disclosure Statements

Ethics approval and consent to participate

Not applicable.

Consent for publication

Not applicable.

Availability of data and materials

The raw data required to reproduce these findings are available in the body and illustrations of this manuscript.

Author's contribution

The authors confirm contribution to the paper as follows: study conception and design: Abu Khalaf, R; theoretical calculations and modeling: Sabbah, D, AlBadawi, G; data analysis and validation: Ikhmais, B, NasrAllah, A. draft manuscript preparation: Awad, M. All authors reviewed the results and approved the final version of the manuscript.

Funding

This work was funded by the Deanship of Scientific Research and Innovation at Al-Zaytoonah University of Jordan (Grant number: 29/06/2024-2025).

Conflicts of interest

The authors declare that there is no conflict of interest regarding the publication of this article.

Acknowledgements

Authors acknowledge the support from the Deanship of Scientific Research and Innovation at Al-Zaytoonah University of Jordan.

References

1] Kaze AD, Santhanam P, Musani SK, Ahima R, Echouffo-Tcheugui JB. Metabolic Dyslipidemia and Cardiovascular Outcomes in Type 2 Diabetes Mellitus: Findings From the Look AHEAD Study. Journal of the American Heart Association. 2021;10(7):e016947.

2] Liu J, Li Y, Ge J, Yan X, Zhang H, Zheng X, Lu J, Li X, Gao Y, Lei L, Liu J, Li J, ESPRIT Collaborative Group. Lowering systolic blood pressure to less than 120 mm Hg versus less than 140 mm Hg in patients with high cardiovascular risk with and without diabetes or previous stroke: an open-label, blinded-outcome, randomised trial. Lancet (London, England). 2024;404(10449):245–255.

3] Su X, Li G, Deng Y, Chang D. Cholesteryl ester transfer protein inhibitors in precision medicine. Clinica chimica acta; international journal of clinical chemistry 2020;510:733–740.

4] Martin SS, Ditmarsch M, Simmons M, Alp N, Turner T, Davidson MH, Kastelein JJP. Comparison of low-density lipoprotein cholesterol equations in patients with dyslipidaemia receiving cholesterol ester transfer protein inhibition. European heart journal. Cardiovascular pharmacotherapy. 2023;9(2):148–155.

5] Nicholls SJ, Nelson AJ. CETP Inhibitors: Should We Continue to Pursue This Pathway?. Current atherosclerosis reports. 2022;24(12):915–923.

6] Dabravolski S, Orekhov N, Melnichenko A, Sukhorukov V, Popov M, Orekhov A. Cholesteryl Ester Transfer Protein (CETP) Variations in Relation to Lipid Profiles and Cardiovascular Diseases: An Update. Current Pharmaceutical Design. 2024;30(10):742-756.

7] Mehta N, Dangas K, Ditmarsch M, Rensen PCN, Dicklin MR, Kastelein JJP. The evolving role of cholesteryl ester transfer protein inhibition beyond cardiovascular disease. Pharmacological Research. 2023;197:106972.

8] Ndrepep G. High-density lipoprotein: a double-edged sword in cardiovascular physiology and pathophysioloy. Journal of Laboratory and Precision Medicine. 2021;6(28):1-24.

9] Kosmas C, DeJesus E, Rosario D, Vittorio T. CETP Inhibition: Past Failures and Future Hopes. Clinical Medicine Insights Cardiology. 2016;10:37-42.

10] Chang B, Laffin LJ, Sarraju A, Nissen SE. Obicetrapib-the Rebirth of CETP Inhibitors?. Current atherosclerosis reports. 2024;26(10):603–608.

11] Schwartz GG, Leiter LA, Ballantyne CM, Barter PJ, Black DM, Kallend D, Laghrissi-Thode F, Leitersdorf E, McMurray JJV, Nicholls SJ, Olsson AG, Preiss D, Shah PK, Tardif JC, Kittelson J. Dalcetrapib Reduces Risk of New-Onset Diabetes in Patients With Coronary Heart Disease. Diabetes care 2020;43(5):1077–1084.
12] Furtado JD, Ruotolo G, Nicholls SJ, Dullea R, Carvajal-Gonzalez S, Sacks FM. Pharmacological Inhibition of CETP (Cholesteryl Ester Transfer Protein) Increases HDL (High-Density Lipoprotein) That Contains ApoC3 and Other HDL Subspecies Associated With Higher Risk of Coronary Heart Disease. Arteriosclerosis, thrombosis, and vascular biology 2022;42(2):227–237.
13] Ballantyne CM, Ditmarsch M, Kastelein JJ, Nelson AJ, Kling D, Hsieh A, Curcio DL, Maki KC, Davidson MH, Nicholls SJ. Obicetrapib plus ezetimibe as an adjunct to high-intensity statin therapy: A randomized phase 2 trial. Journal of clinical lipidology. 2023;17(4):491–503.
14] Jarab A, Alefishat E, Al-Qerem W, Mukattash T, Al-Hajjeh D. Lipid control and its associated factors among patients with dyslipidaemia in Jordan. International Journal of Clinical Practice. 2021;75(5):e14000.
15] Abu Khalaf R, Sheikha G, Bustanji Y, Taha M. Discovery of new cholesteryl ester transfer protein inhibitors via ligand-based pharmacophore modeling and QSAR analysis followed by synthetic exploration. European Journal of Medicinal Chemistry. 2010;45(4):1598-1617.
16] Abu Sheikha G, Abu Khalaf R, Melhem A, Albadawi G. Design, synthesis, and biological evaluation of benzylamino-methanone based cholesteryl ester transfer protein inhibitors. Molecules. 2010;15(8):5721-5733.
17] Abu Khalaf R, Sheikha G, Al-Sha'er M, Albadawi G, Taha M. Design, synthesis, and biological evaluation of sulfonic acid ester and benzenesulfonamide derivatives as potential CETP inhibitors. Medicinal Chemistry Research. 2012;21(11):3669-3680.
18] Abu Khalaf R, Abd El-Aziz H, Sabbah D, Albadawi G. Abu Sheikha G. CETP Inhibitory Activity of Chlorobenzyl Benzamides: QPLD Docking, Pharmacophore Mapping and Synthesis. Letters Drug Design and Discovery. 2017;14(12):1391-1400.
19] Abu Khalaf R, Al-Rawashdeh S, Sabbah D, Abu Sheikha G. Molecular docking and pharmacophore modeling studies of fluorinated benzamides as potential CETP inhibitors. Medicinal Chemistry. 2017;13(3):239-253.
20] Abu Khalaf R, Sabbah D, Al-Shalabi E, Bishtawi S, Albadawi G, Abu Sheikha G. Synthesis, Biological Evaluation, and Molecular Modeling Study of Substituted Benzyl Benzamides as CETP Inhibitors. Archive der Pharmazie. 2017;350(12):1700204.
21] Abu Khalaf R, NasrAllah A, Jarrar W, Sabbah D. Cholesteryl Ester Transfer Protein Inhibitory Oxoacetamido-Benzamide Derivatives: Glide Docking, Pharmacophore Mapping, and Synthesis, Brazilian Journal of Pharmaceutical Science. 2022;58:e20028.
22] Abu Khalaf R, Awad M, Al-Qirim T, Sabbah D. Synthesis and Molecular Modeling of Novel 3, 5-Bis (trifluoromethyl) benzylamino Benzamides as Potential CETP Inhibitors. Medicinal Chemistry. 2022;18(4):417-426.
23] Abu Khalaf R, Sabbah D, Al-Shalabi E, Ikhmais B, Naser W, Albadawi G. Fluorinated Benzyloxalamides: Glide Docking, Pharmacophore Mapping, Synthesis and In Vitro Evaluation as Potential Cholesteryl Ester Transfer Protein Inhibitors. Indian Journal of Pharmaceutical Science. 2022;84(6):1476-1487.
24] Abu Khalaf R, Abusaad A, Al-Nawaiseh B, Sabbah D, Albadawi G. Synthesis, Molecular Modeling and Biological Evaluation of Novel Trifluoromethyl Benzamides as Promising CETP Inhibitors. Current Computer-Aided Drug Design. 2024;20(5):564-574.
25] Liu S, Mistry A, Reynolds J, Lloyd D, Griffor M, Perry D, Ruggeri R, Clark R, Qiu X. Crystal structures of cholesteryl ester transfer protein in complex with inhibitors. Journal of Biological Chemistry. 2012;287:37321-37329.
26] Schrödinger. Protein Preparation Wizard, Maestro, Macromodel, QPLD-dock, and Pymol. Schrödinger, LLC, Portland, OR, U.S.A. 97204; 2022.
27] Friesner R, Banks J, Murphy R, Halgren T, Klicic J, Mainz D, Repasky M, Knoll E, Shelley M, Perry J, Shaw D, Francis P, Shenkin P. Glide: A new approach for rapid, accurate docking and scoring. 1. Method and assessment of docking accuracy. Journal of Medicinal Chemistry. 2004;47:1739-1749.
28] Friesner R, Murphy R, Repasky M, Frye L, Greenwood J, Halgren T, Sanschagrin P, Mainz D. Extra precision glide: Docking and scoring incorporating a model of hydrophobic enclosure for protein-ligand complexes. Journal of Medicinal Chemistry. 2006;49:6177-6196.
29] Genheden S, Ryde U. The MM/PBSA and MM/GBSA methods to estimate ligand-binding affinities. Expert Opinion on Drug Discovery. 2015;10(5):449-461.
30] Tuccinardi T. What is the current value of MM/PBSA and MM/GBSA methods in drug discovery? Expert Opinion on Drug Discovery. 2021;16(11):1233-1237.
31] MOE. The Molecular operating, Environment Chemical Computing Group, Inc Montreal, Quebec Canada; 2020.